Journal of Hydrology 637 (2024) 131379

Contents lists available at ScienceDirect

Journal of Hydrology

journal homepage: www.elsevier.com/locate/jhydrol

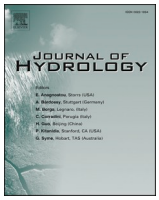

Research papers

Flux tracking of groundwater via integrated modelling for abstraction management

Leyang Liu [a,*], Marco Bianchi [b], Christopher R. Jackson [b], Ana Mijic [a]

[a] Department of Civil and Environmental Engineering, Imperial College London, London, United Kingdom
[b] British Geological Survey, Keyworth, Nottingham, United Kingdom

ARTICLE INFO

This manuscript was handled by Corrado Corradini, Editor-in-Chief, with the assistance of Nick Engdahl, Associate Editor

Keywords:
Groundwater abstraction
Integrated modelling
Flux tracking
Surface water-groundwater interaction
Abstraction management
System diagnosis

ABSTRACT

In systems where surface water and groundwater interact, management of the water resource often involves conflicting objectives between water supply and baseflow maintenance. Balancing such objectives requires understanding of the role of groundwater in integrated water systems to inform the design of an efficient strategy to minimise abstraction impacts. This study first develops a reduced-complexity, processed-based groundwater model within the water systems integration modelling framework (WSIMOD). This model is applied to the Lea catchment, UK, as a case study and evaluated against monitored groundwater level and river flow data. A flux tracking approach is developed to reveal the origins of both river baseflow at a critical assessment point and abstracted groundwater across the systems. The insights obtained are used to design two strategies for groundwater abstraction reduction. Results show that the model has good performance in simulating the groundwater and river flow dynamics. Three aquifer bodies that contribute the most to the river baseflow in the dry season at the assessment point are identified; contributions being 17 %, 15 %, and 5 %. The spatial distribution of abstracted groundwater originating from these aquifer bodies is illustrated. Compared to the default equal-ratio reduction, the strategy prioritising abstraction reduction in these three aquifer bodies increases a similar amount of baseflow (13 %) by reducing much less abstraction (23 %). The other strategy, which further decreases abstraction in the adjacent aquifer bodies, increases more baseflow (16 %) with a similar abstraction reduction (30 %). Both strategies can more efficiently improve the baseflow. The flux tracking approach can be further implemented to trace water from other origins, including runoff, stormwater, and wastewater, to enable coordinated management for better systems-level performance.

1. Introduction

Groundwater interactions with human and environmental systems are an important component of the catchment water cycle (Li et al., 2018). Groundwater may support river baseflow as well as receive leakage from surface water bodies including rivers, lakes, and wetlands (Brunner et al., 2017; Lapworth et al., 2021). Because of these interactions, it has been reported that significant groundwater abstractions can both reduce groundwater levels and cause streamflow depletion in many catchments worldwide (Chen and Yin, 2001; Zipper et al., 2019). Managing abstractions for groundwater use and river flow maintenance is therefore challenging (Xevi and Khan, 2005).

To address this challenge in the UK, low flow conditions as well as the impacts from groundwater abstraction have been evaluated at certain assessment points, which are often gauging stations or the confluence between two rivers (Environment Agency, 2020). Hands-off flows (HoF) and hands-off level (HoL) constraints, the river flows and groundwater levels below which the abstraction should be reduced or suspended, can be set to protect low river flows in dry periods (Environment Agency, 2019). The Environment Agency of England has also been reforming existing abstraction licences to further decrease the environmental pressures and prevent future deterioration (Department for Environment, Food and Rural Affairs, 2019). However, reducing groundwater abstraction for public water supply or irrigation, may cause trade-offs between socio-economic development and environmental benefits (Department for Environment, Food and Rural Affairs, 2021; Schwarz and Mathijs, 2017; Wang et al., 2022). It is thus important to determine where and by how much the abstraction should be reduced to increase the baseflow with minimal impact on water use, especially under pressures such as climate change and population

* Corresponding author.
E-mail address: leyang.liu16@imperial.ac.uk (L. Liu).

https://doi.org/10.1016/j.jhydrol.2024.131379
Received 6 January 2024; Received in revised form 27 April 2024; Accepted 7 May 2024
Available online 27 May 2024

growth. This requires an understanding of the interactions between groundwater and the other components in integrated water systems.

To reveal the interactions, catchment hydrological modelling has been widely adopted with a focus on simulating large-scale processes near the land surface (Barthel, 2006). Groundwater bodies, along with soil water storage and surface water runoff, are generally represented by parsimonious linear reservoirs (e.g., HBV (Bergström and Lindström, 2015), VIC (Gao et al., 2010), mHM (Samaniego et al., 2011), IHACRES (Ivkovic, 2006), GR4J (Perrin et al., 2003) etc.). The behaviour of the linear reservoirs is commonly described by parameters such as recession coefficient (Jukić and Denić-Jukić, 2009) and residence time (Knoben, 2019), which require significant calibration to fit to observed river flow series (Jing et al., 2018). This conceptualisation has advantages in quickly modelling groundwater contribution to streamflow seasonal dynamics by simulating aquifers receiving recharge from the upper soil and discharging baseflows to rivers. However, the simplicity of the conceptualisation cannot provide adequate information for management, especially regarding human water use; borehole abstractions are not included (Jukić and Denić-Jukić, 2009; Mackay et al., 2014), or their impacts cannot be accurately evaluated due to lack of physically-based representations of lateral groundwater flows (e.g., SWAT (Neitsch et al., 2011), HYPE (HYPE Model Documentation, 2021)), which can be significant (Oldham et al., 2023).

Numerical groundwater flow models, as an alternative approach, discretise the geological layers into computational grids and simulate piezometric heads and subsurface fluxes in aquifers by solving 2D or 3D partial differential equations (PDEs) governing flow in porous media (e.g., MODFLOW (Hill et al., 2000) and FEFLOW (Diersch, 2013)). These models have also been coupled with the PDEs describing overland processes to simulate detailed interactions with surface water (e.g., CATHY (Camporese et al., 2010), ParFlow (Kollet and Maxwell, 2006), IRENE (Spanoudaki et al., 2009)). Since these models can take into account the geological complexity and the heterogeneity of subsurface hydraulic properties (e.g., hydraulic conductivity, confined/unconfined storage coefficients), they can provide more physical details of interactions such as how abstraction affects the groundwater flow (Lancia et al., 2020; Xu et al., 2009) and regional gains/losses between surface and groundwater bodies (Baalousha, 2012; Valerio et al., 2010). However, computational demand and simulation time are significantly increased, which can make it difficult to explore and design optimal management strategies (Jing et al., 2018).

Coupling hydrological and groundwater models into an integrated framework has been attempted to simulate holistic systems interactions involved with groundwater (e.g., HBV-MODFLOW (Gaiser et al., 2008), VIC (Scheidegger et al., 2021; Sridhar et al., 2018), SWAT-MODFLOW (Kim et al., 2008) CWatM-MODFLOW (Guillaumot et al., 2022), mHM-OGS (Jing et al., 2018), MIKE SHE (Ma et al., 2016), SHETRAN (Ewen et al., 2000), etc.). Though it has gained success in reproducing the spatio-temporal behaviour of the catchment hydrological cycle, it presents complications given the mix of scales of the processes simulated (Barthel, 2006), sometimes incompatible model structures (Hughes et al., 2010), as well as greater uncertainty arising from the increased number of parameters (Prucha et al., 2016). Moreover, coupled numerical models still require long simulation times (Haque et al., 2021) and therefore their application to the design of water management strategies is challenging. The urban water cycle, including supply and drainage systems as well as wastewater treatment plants, has not been incorporated.

To address these challenges, WSIMOD, an integrated modelling framework tailored for water management, has been developed, which can flexibly accommodate various representations of water system components as well as their interactions (Dobson et al., 2023). However, its current parsimonious groundwater representation based on conceptual water tanks governed by residence time should be improved to simulate bi-directional river-aquifer interactions and lateral flows. This could be achieved by introducing physical variables (e.g., water head) and parameters (e.g., transmissivity) lumped at a catchment scale, to enable the simulations with low complexity and computational demand (Barrett and Charbeneau, 1997; Griffiths et al., 2023; Mackay et al., 2014). Such an integrated modelling framework can provide extensive information on fluxes in the water systems, helping to understand how water routes to an assessment point in the river through surface and subsurface processes.

The concept of water age has been adopted to estimate the travel time that rainfall water parcels undertake in the mixing, storage, and transport to the catchment outlet (Botter et al., 2010; McDonnell et al., 2010; Rinaldo et al., 2011). Its probability density function, referred to as 'transit time distributions (TTDs)', characterises the overall catchment water transport behaviour (Hrachowitz et al., 2013; Kirchner, 2016) and has implications for water pollution assessment (Eberts et al., 2012; Kumar et al., 2020). For evaluating TTDs, flux tracking assumes the complete mixing of water with different ages in the conceptual storages (e.g., soil water and groundwater) and has been applied with distributed hydrological modelling (Jing et al., 2021; Remondi et al., 2018). This approach has successfully revealed increased water age from surface to subsurface. Alternatively, particle tracking has been implemented within numeric groundwater models to evaluate the transit time of water from a discretised cell to its discharge point (e.g., abstraction boreholes, springs) and illustrate the detailed pathline trajectories (Gusyev et al., 2014; Jing et al., 2021; Kaandorp et al., 2018; Kaandorp et al., 2021). However, due to the high computational demand from physically based models, both approaches are normally studied on small scales (Remondi et al., 2018). Although TTDs can reveal the catchment temporal residence-transport dynamics, they do not indicate the spatial locations where the water in conceptual storages comes from, defined as 'origins of water fluxes' in this study. Pathline trajectories can depict the origins of a water parcel and indicate the proportions of fluxes from different origins in a water body, but this can require additional parameterisation (i.e., of porosity) and significant post-processing of model output. Knowing such information helps to identify prioritised locations and design the target for groundwater abstraction reduction to maintain baseflows in rivers, especially in large catchment systems with complicated processes. A new flux tracking approach is thus needed to be developed and facilitated by an integrated modelling framework with reduced complexity and faster simulation.

To understand the role of groundwater in integrated water resources management, this study first develops a reduced-complexity, process-based groundwater module driven by physical variables and parameters and incorporates it into WSIMOD. The resulting new WSIMOD-GW model is then applied to a large catchment system to holistically simulate groundwater interactions with different human and environmental components. A novel flux tracking approach is also integrated into WSIMOD-GW to reveal the origins of both baseflows in the river at an assessment point and abstracted groundwater across the whole catchment as a system diagnosis. Based on the insights, abstraction reduction strategies are then designed and tested to manage the trade-offs between water use and baseflow improvement.

2. Study area

The River Lea catchment in southern England (UK), is the case study for this work (Fig. 1). The region includes 35 sub-catchments derived from the Water Framework Directive (WFD) River Waterbody Catchments Cycle 2 (Environment Agency, 2021), comprising a total area of 1,386 km^2. The land cover is predominantly rural, with 19 % categorised as winter wheat and 17 % as grass, a significant proportion of which is located in the north-east (Morton et al., 2022). Populated urban or suburban areas are mainly located in the north-west (Luton) and south (London), accounting for 327 km^2 in total. Two tributaries from the north-west (mean flow 3.2 m^3/s) and the north-east (1.4 m^3/s) join at the middle region, forming the Lower River Lea (mean flow 5.6 m^3/s) (UK Centre for Ecology and Hydrology, 2020). Before flowing into the

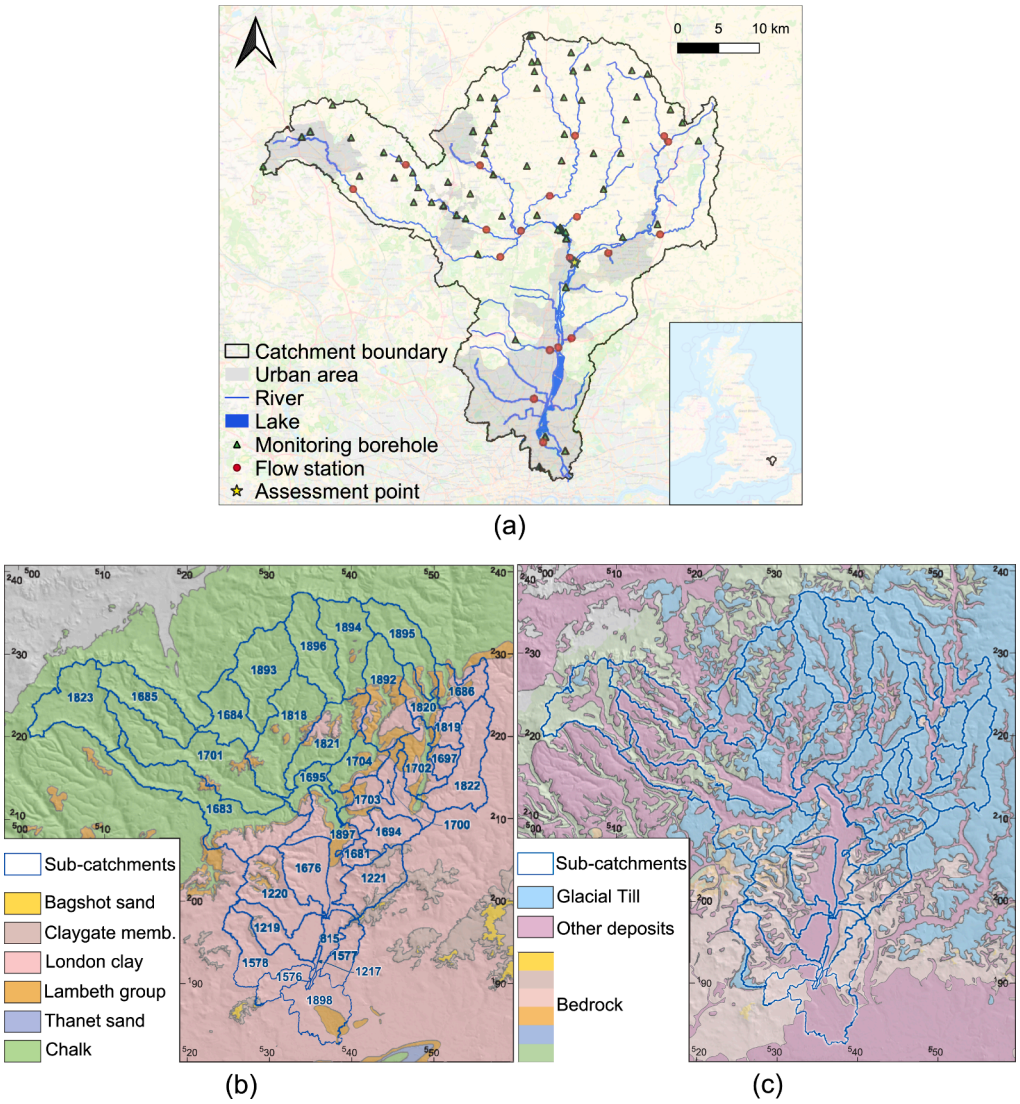

Fig. 1. Information on land cover, water bodies, and monitoring stations (boreholes for groundwater levels and locations for river flow monitoring) in the Lea catchment (a), sub-catchment Water Framework Directive (WFD) ID and bedrock geology (b), and superficial geology (c). This figure contains British Geological Survey data © UKRI 2023 and Ordnance Survey data © Crown copyright and database right 2023.

River Thames, the River Lea interacts extensively with lakes, wetlands, reservoirs, and canals and numerous weirs are present, which results in a complex water system. The Upper and Middle River Lea receives significant effluent from many wastewater treatment plants, which has a great negative impact on aquatic ecology, especially during summer (Harries et al., 1996). The hydrogeological setting is characterised by the presence of the unconfined Chalk aquifer in the northern part of the catchment, which is overlain by low permeability London Clay Formation in the south and south-east. On top of these bedrock units, low permeability Quaternary glacial till covers much of the east of the study area. A variety of other unconsolidated superficial deposits also cover the area, e.g. river valley gravels and river alluvium, but these are generally permeable and so have been categorised as'Other deposits' in Fig. 1(c). The presence of the London Clay and the glacial till is responsible for inducing confined conditions in parts of the Chalk aquifer (Fig. 1(b-c)). Groundwater abstraction from the Chalk aquifer is widely distributed throughout the whole area, accounting for at least 55 % of the total water supply (Marsili et al., 2023).

3. Methodology

The updated version (WSIMOD-GW) of the Water Systems Integration Modelling Framework (WSIMOD) is introduced first. This incorporates a process-based groundwater module to represent bi-directional river-aquifer interactions as well as groundwater lateral flows (Section 3.1). The data used for model set-up and validation in the Lea catchment is then presented. A new flux tracking approach that reveals the origin of water is then described using a conceptual example (Section 3.2). Finally, the insights obtained by the flux tracking are used to design strategies for groundwater abstraction reduction to improve baseflow at a critical assessment point (Section 3.3).

3.1. WSIMOD-GW

3.1.1. The Water Systems Integration Modelling Framework (WSIMOD)

WSIMOD is an open-source Python package for understanding water systems interactions and designing water management strategies (Dobson et al., 2023). It has been applied to several regions in the UK and successfully discovered useful systems mechanisms that can facilitate more effective water management, including integrated urban supply-

drainage operation (Dobson and Mijic, 2020), urban–rural pollutant loads reduction (Liu et al., 2023a), nature-based solution planning (Liu et al., 2023b). The variety and complexity of the water budget components in the Lea catchment (Section 2) make it an ideal modelling case for the application of WSIMOD.

WSIMOD simulates multiple components of the water cycle in both urban (built-up land, water supply pipes, domestic demand, wastewater treatment works (WWTWs), storm and foul sewers) and rural environments (soil with different vegetations), as well as water bodies (rivers and aquifers) (Fig. 2(a)). The components are designed to interact with each other, allowing for a flexible representation of the water cycle to accommodate different configurations. A default configuration at a sub-catchment scale includes interactions between rural land and water bodies (① surface and subsurface runoffs and ⑦ recharge in Fig. 2(a)), urban infrastructure and water bodies (④ surface and groundwater abstractions, ⑧ pipe leakages, ② storm and wastewater discharge), within the urban infrastructure (③ drainage pipe misconnections), and water bodies (⑤ upstream–downstream river flow discharge and ⑨ baseflow). Detailed information on model representations of the default components and interactions can be found in the model documentation (Dobson, 2022). To enhance the subsurface process representations, river leakage into aquifers (⑨) and groundwater lateral flows (⑥) were added in this study, along with a revised conceptualisation of the groundwater component (Section 3.1.2). Though groundwater abstraction for agricultural irrigation can be simulated, it was not included in this case study given the small irrigated area (1.1 % of the cropland in

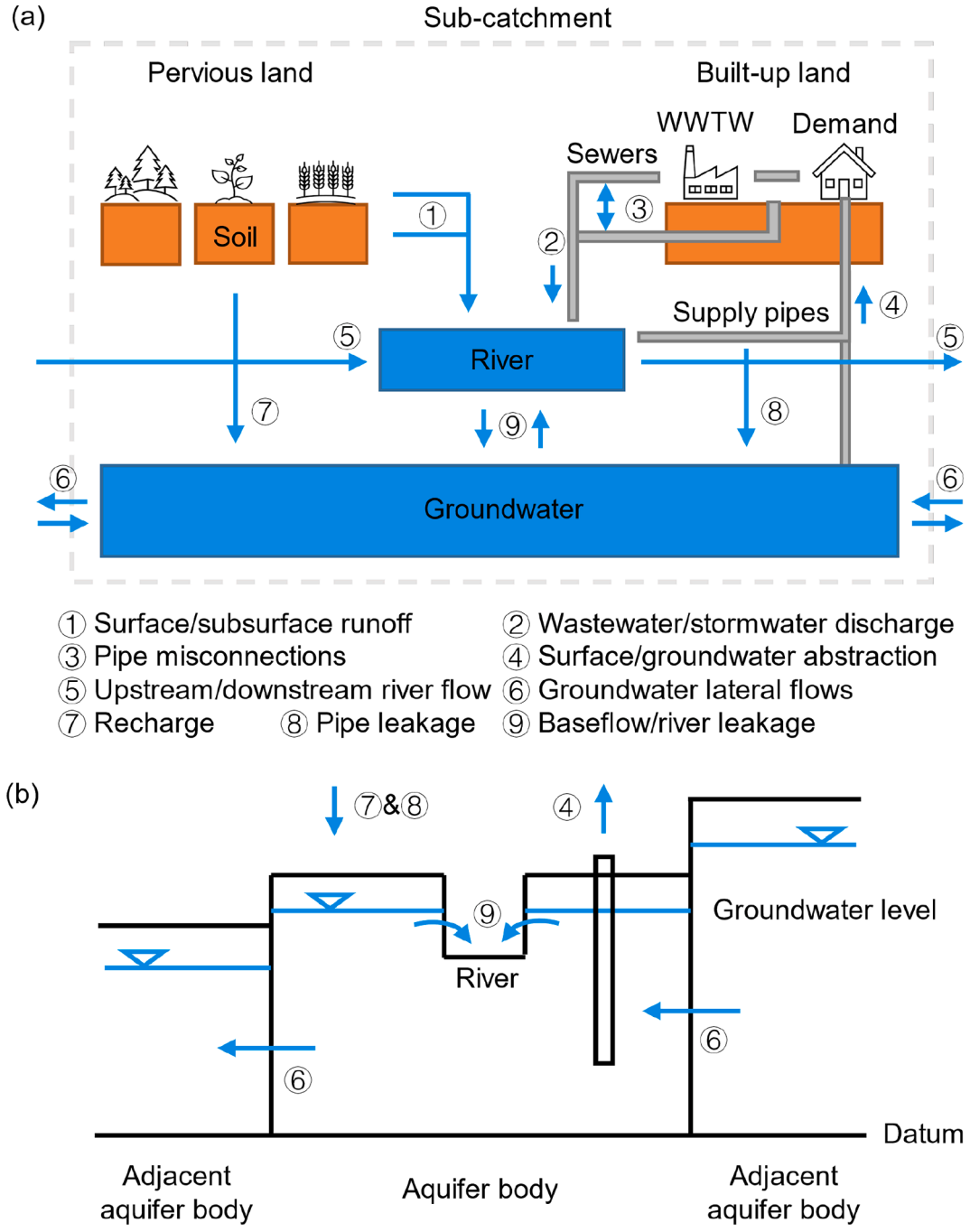

Fig. 2. A schematic diagram of the integrated water cycle in sub-catchments modelled by the WSIMOD (a) and a conceptualisation of aquifer bodies via a reduced-complexity process-based approach (b).

the Upper Lea (Knox et al., 2017)).

3.1.2. A reduced complexity process-based groundwater module

The groundwater component within each sub-catchment, termed an 'aquifer body', in the original WSIMOD is represented by a conceptual tank with storage volume as its only state variable (Fig. S7 in Supplementary Material). The baseflow to rivers at each time step is generated by dividing storage using a parameter of residence time. The riverbed leakage and groundwater lateral fluxes are simulated based on user-specified timeseries input.

In this work, it is further developed to enhance the representation of subsurface processes (Fig. 2(b)). To avoid significantly increasing modelling complexity, the conceptual tank representation remains, but more physical variables are introduced as follows.

$$V = SAh \tag{1}$$

where V is the storage volume of the aquifer body (m^3), S is the storage coefficient (−), A is the area of sub-catchment (m^2), and h is the groundwater level (m).

The interactions between the aquifer body and the river in the sub-catchment (⑨) are driven by the difference between the groundwater level and the water level in the river or stage elevation (Eq. (2). At a sub-catchment scale, the river level is approximated by the riverbed elevation, given that fluctuations of the river level are generally negligible compared to seasonal variations of groundwater levels within the aquifer body. If the groundwater level is larger than the riverbed elevation, then the river receives baseflow from the aquifer body; otherwise, a leakage flux is generated from the river to the aquifer body through the riverbed. The flux between the river and the aquifer body can then be quantified by the following equation (Anderson et al., 2015).

$$Q_{gw-river} = c_{riverbed} LW(\bar{z}_{river} - h) \tag{2}$$

where $Q_{gw-river}$ is the flux between groundwater and river (m^3/d), $c_{riverbed}$ is the riverbed conductance (day^{-1}), L and W are the total length and width of the river channel within the sub-catchment (m), and $\bar{z}_{river}$ is the mean elevation of the river (m).

Groundwater lateral flows (⑥) are driven by the difference in water head between adjacent aquifer bodies (Eq. (3a) and (3b).

$$Q_{gw-gw} = \sum_{i=1}^{n} c_{gw,i}(h_i - h) \tag{3a}$$

$$c_{gw,i} = KA_i/L_i \tag{3b}$$

where Q_{gw-gw} is the total groundwater lateral flow across the boundaries between the reference aquifer body and adjacent bodies (m^3/day), $c_{gw,i}$ is the conductance between the reference aquifer body and the adjacent body i (m^2/day), h_i is the groundwater head in the adjacent aquifer body i (m), K is hydraulic conductivity (m/day), A_i is the cross-sectional area between the aquifer body and the adjacent body i (m^2), and L_i is the distance between the centroids of adjacent aquifer bodies (m).

The aquifer body can also receive the fluxes from the upper soil, including both natural recharge (⑦) and pipe leakages (⑧) that are simulated in the other components in the WSIMOD, and be abstracted via boreholes (④). A mass balance calculation is performed at each timestep to update the new groundwater storage (Eq. (4)).

$$\Delta V = Q_{gw-river} + Q_{gw-gw} + R - P \tag{4}$$

where R is the sum of natural recharge and pipe leakages (m^3/day), and P is the sum of groundwater abstraction within the sub-catchment (m^3/day).

Confined aquifer bodies are assumed to have no interactions with the upper soil (⑦⑧) and rivers (④), which are disabled in the simulation.

3.1.3. Data

WSIMOD uses publicly available datasets, including hydroclimatic, land cover, population, and vegetation parameters, for set-up in the UK catchments, with detailed information described in Liu et al. (2021, 2023). Data specifically used for the groundwater set-up and validation is summarised in Table 1. Storage coefficient is set using reference values recommended by Allen et al. (1997), with 0.01 and 0.001 for unconfined and confined aquifers in the UK, respectively. Riverbed elevation (in meters above sea level (mASL)) is evaluated by overlaying the river network with the LIDAR Composite Digital Terrain Model (DTM) (Environment Agency, 2023). Aquifer conductance between adjacent groundwater bodies is based on the calibrated hydraulic conductivity value for the Chalk aquifer (3.05 m/d in this area), in the national-scale numerical British Groundwater Model (BGWM) (Bianchi et al., 2024) and the thickness of the Chalk aquifer at each grid cell. The BGWM also provides boundary conditions in the form of monthly averaged lateral groundwater flows. Monthly average groundwater abstractions at boreholes are obtained from the Environment Agency under a data-sharing agreement and are aggregated within each sub-catchment. The model simulated the period from 1 January 2000 to 31 December 2015 at a daily time step. The whole simulation lasts around 2 h at a desktop using an Intel Xeon W-2102 CPU with 64 GB RAM and a NVIDIA Quadro P1000 GPU.

The model is evaluated against observed river flow from the National River Flow Archive (NRFA) (UK Centre for Ecology and Hydrology, 2020) and groundwater level time series from the Hydrology Data Explorer (Department for Environment Food and Rural Affairs, 2023), respectively. Locations of observations (gauges and boreholes) are shown in Fig. 1(a). For evaluation of the model accuracy in reproducing observed river flows, we adopt Nash-Sutcliffe Efficiency (NSE), which is a common metric used for hydrological model validation (Moriasi et al., 2007). For evaluating the accuracy of the simulated groundwater levels, the results are compared to measured groundwater levels in boreholes averaged within a sub-catchment. For facilitating the comparison between simulated values, which are representative of the entire sub-catchment area, and the observed values, which instead represent local conditions mostly along the rivers (Fig. 1(a)), both are transformed into a monthly standardised groundwater level index (SGI) (Bloomfield and Marchant, 2013). The Pearson's correlation coefficient between both SGIs is calculated to quantitatively evaluate the consistencies between the simulated and observed temporal standardised groundwater level fluctuations. For a complete model evaluation, the mean absolute error (MAE) is also calculated to estimate the discrepancies in absolute values of the simulated and observed groundwater levels lumped at each sub-catchment, though the latter of which are not representative enough due to the locations and limited number of boreholes (Table S1 in Supplementary Material).

As an integrated modelling tool, WSIMOD involves a significant number of parameters describing various processes in subsystems (Dobson, 2022). A formal calibration may obtain similar high-performance metrics resulting from significantly different sets of parameter values (Dobson et al., 2021). To constrain the modelling uncertainties in this study, parameters are evaluated using as much of the best publicly available evidence as possible (see Table 1 for groundwater and Liu et al. (2023) for the other subsystems). Those parameters without enough available evidence are manually adjusted to fit the observed data, including soil field capacity, partitioning coefficients for surface, subsurface runoffs and recharge, runoff routing time, and riverbed conductance. This practice might not result in the best performance metrics but has been demonstrated to provide insights into systems responses to parameter values (Liu et al., 2023a,b), which ultimately better serves this study's purpose in understanding system interactions.

3.2. Flux tracking of groundwater

To depict the groundwater movement and its interactions with rivers, a flux tracking approach is developed based on the simulated

Table 1
Data for groundwater set-up and validation in WSIMOD-GW.

Data	Variables	Source	Temporal information	Spatial information
Ground-water model set-up	Groundwater abstraction	Monthly historical borehole abstraction	2000–2015	Borehole
	Aquifer conductance	The British Groundwater Model (BGWM) (Bianchi et al., 2024)	–	Sub-catchment boundaries
	Boundary lateral flows		Long-term monthly averages	Catchment boundaries
	Storage coefficient	Allen et al. (1997)	–	Aquifer
	River bed elevation	Ordnance Survey Open Rivers	–	River network
		LIDAR Composite DTM (Environment Agency, 2023)	2022	10 m
Model validation	Groundwater level	Hydrology Data Explorer (Department for Environment Food & Rural Affairs, 2023)	2000–2015 monthly	71 boreholes
	River flow	National River Flow Archive (NRFA) (UK Centre for Ecology and Hydrology, 2020)	2000–2015 daily	20 stations

water fluxes in the system. The approach is illustrated using a conceptual example in Fig. 3.

The approach begins with setting initial conditions by allocating the groundwater in the aquifer body (AB) to the local system. For example, the initial storage (V_0) is fully tagged with AB *a* at time t_0 (Fig. 3(a)). During the timestep Δt, the flux tracking algorithm identifies the origins of fluxes into aquifer bodies and their proportions. In the example given (Fig. 3(b)), two fluxes are identified entering the AB *a*: recharge $q_{in,1}$ allocated to the local system and fully tagged with AB *a*, and lateral flows $q_{in,2}$ from two adjacent aquifer bodies *b* ($q_{in,2,b}$) and *c* ($q_{in,2,c}$). The composition of storage, indicated by the percentages of water from different origins, is updated in aquifer bodies. In Fig. 3(c), AB *a* now contains a total volume of $V_0 + q_1 + q_2$, with a proportion of p_a from the local system and p_b and p_c from AB *b* and *c*, respectively.

The water from different origins is assumed to fully mix in aquifer bodies, resulting in the outflows (q_{out}) sharing the same composition with the groundwater storage (p_a, p_b, and p_c). The example shows three fluxes leaving the AB *a* (Fig. 3(d)): the groundwater abstraction $q_{out,1}$, baseflow to the river $q_{out,2}$, and the lateral flows to other aquifer bodies $q_{out,3}$. Finally, the water storage in the next time step (V_1) is calculated by removing the outflows, and the proportions of water origins are updated (Fig. 3(e)).

These steps are repeated at each timestep based on the simulated results of water storage and fluxes. It is noted that lateral flows crossing the boundaries into the study region are tagged with the name of the receiving aquifer bodies, as the fluxes cannot be traced back to their original aquifer body. Fluxes in rivers that do not come from groundwater, including surface and subsurface runoffs, storm, and wastewater, are tagged as *'Other'*. As a result, the composition of water in the fluxes and storages within the catchment system can be obtained during the whole simulation period.

To eliminate the impacts of initial conditions on the results, a six-year spin-up period is set to allow the compositions of water from different origins in aquifer bodies to reach dynamic equilibrium (Fig. S6 in Supplementary Material). The results after this spin-up period were then analysed, from 2006 to 2015.

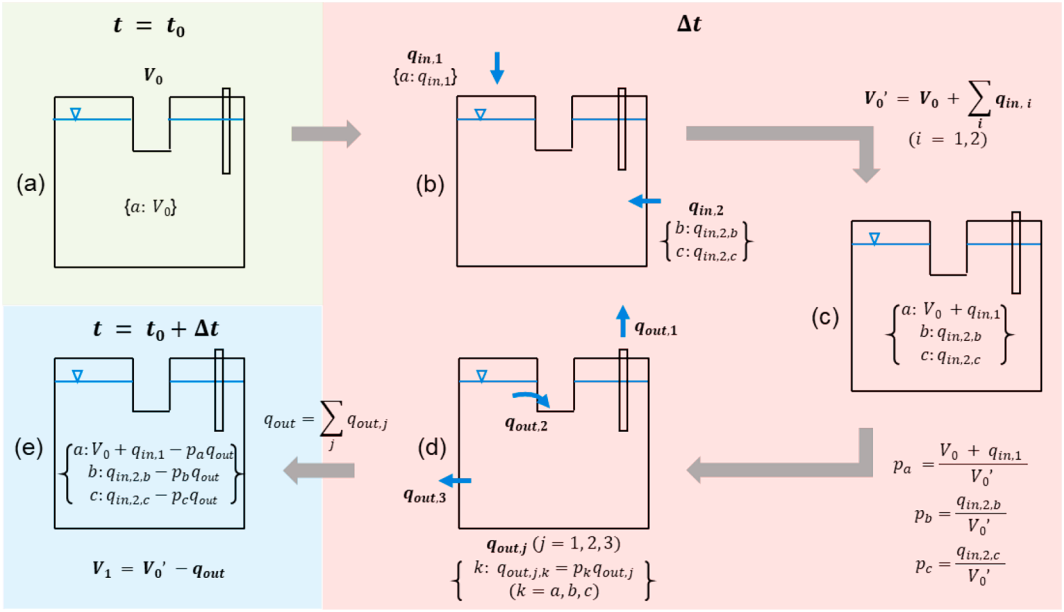

Fig. 3. A conceptual example of the flux tracking approach for an aquifer body (named *a*) at a time step (from t_0 to $t_0 + \Delta t$), to reveal the origin of water in rivers and aquifer bodies. V_0 is the initial water storage in aquifer body *a*; during the time step Δt, $q_{in,1}$ is the recharge from the upper soil, $q_{in,2}$ is the sum of groundwater lateral flows from the adjacent aquifer bodies *b* ($q_{in,2,b}$) and *c* ($q_{in,2,c}$), V_0' is the water storage after accounting for inflow fluxes, p_a, p_b, and p_c are the proportions of water storage originating from aquifer bodies *a*, *b*, and *c*, respectively, $q_{out,1}$ is the groundwater abstraction, $q_{out,2}$ is the baseflow to the river, and $q_{out,3}$ is the sum of groundwater lateral flows to the other adjacent aquifer bodies, their components originating from aquifer bodies *a*, *b*, and *c* are denoted using $q_{out,j,k}$, q_{out} is the total outflow as a sum of these three fluxes, and V_1 is the water storage at $t_0 + \Delta t$.

3.3. Groundwater abstraction reduction strategies

The insights obtained from the flux tracking are used to design hypothetical groundwater abstraction reduction schemes for river flow management at a critical assessment point. This study selects the Feildes Weir as the assessment point (Fig. 1(a)), which has been listed by earlier research as an important location to characterise floods (Segond et al., 2007), droughts (Marsh and Cole, 2006), and water quality (Flynn et al., 2002) in the Lea catchment. This assessment point aggregates the flows from the whole Upper Lea catchment, where the unconfined Chalk aquifer has direct interactions with the rivers (Fig. 1(b)). The baseflow conditions at this point are important for the downstream reservoirs and lakes that supply significant amounts of surface water to North London and support the wetland ecosystems in Lower Lea, especially during the dry season. The baseflow also dilutes a significant amount of wastewater discharged nearby thus improving the river water quality and ecology (Flynn et al., 2002).

Three hypothetical groundwater abstraction schemes are developed and depicted using a conceptual example (Fig. 4). This example includes aquifer bodies *a*, *b*, and *c* that all generate baseflows to an assessment point but have different water compositions. Without the information about the river flow origins, groundwater abstraction is firstly assumed to be reduced by the same percentage at the boreholes in the sub-catchments upstream of the assessment point, resulting in an 'equal-ratio reduction' strategy. A 32 % reduction ratio is set according to the Affinity Water Resources Management Plan (Affinity Water, 2022).

In contrast, flux tracking reveals the proportions of the baseflow from different aquifer bodies at the assessment point in the dry season (from May to August) (Section 4.2.1). Those aquifer bodies that contribute to significant proportions, termed 'prioritised aquifer bodies', should be protected by reducing the on-site groundwater abstractions. A 'prioritised reduction' strategy is thus designed, where all aquifer bodies with a contribution >5 % (e.g., AB *a* and *b* in Fig. 4) will be selected for 100 % reduction, while the rest of the abstractions (e.g., in AB *c*) will remain unchanged. We note that the 5 % threshold is arbitrary and its impacts on the results could be explored further.

Finally, flux tracking can evaluate the origins of groundwater abstraction in each sub-catchment (Section 4.2.2). For example, the water abstracted from AB *a* contains 30 % and 20 % water from adjacent AB *b* and *c*, respectively (Fig. 4). With such information, instead of only reducing the local abstraction, abstractions from all the boreholes that can access the water originating from the prioritised aquifer bodies could be reduced. This informs the design of a 'prioritised and adjacent reduction' strategy: groundwater abstraction in a sub-catchment should reduce by the proportions of water it contains originating from the prioritised aquifer bodies. In the provided example, the groundwater abstractions in the sub-catchments *a* and *b* contain 80 % and 95 % of water originating from the prioritised AB *a* and *b* in total, respectively. The reduction in abstraction should align with these two specified percentages, respectively. Though aquifer body c is not designated as a prioritised aquifer body, the boreholes there can still have access to water from aquifer body *a* at a rate of 20 %, necessitating a reduction in abstraction by this percentage.

In all the strategies, the reduced groundwater abstraction is assumed to be complemented by water resources from the external region to satisfy the historical water demand. We also note that this study compares these three strategies for exploring how flux tracking results can be used to inform the design of more efficient groundwater abstraction reduction strategies. As a potential experiment, the optimal amount and locations of groundwater abstraction reduction could be searched via optimisation techniques and compared with these strategies to obtain further management insights.

The strategies' performance is evaluated using metrics that represent the trade-off objectives between water companies and regulatory bodies. The first metric is the average daily groundwater abstraction within the whole catchment system. This reflects how different strategies of groundwater abstraction reduction can affect the water supply service provision and potentially the resilience of domestic water use, which may be in water companies' interests. The second metric is the mean river flow change in the dry season at the assessment point during the simulation period. This reveals the degree of baseflow improvement, which regulatory bodies such as the Environment Agency of England seek to enhance.

4. Results

4.1. Model evaluation

4.1.1. Groundwater level

The observed and simulated standardised groundwater level index (SGI) shows a consistent temporal pattern in most of the sub-catchments with available monitoring data (Fig. 5). The 50 % of the 20 sub-

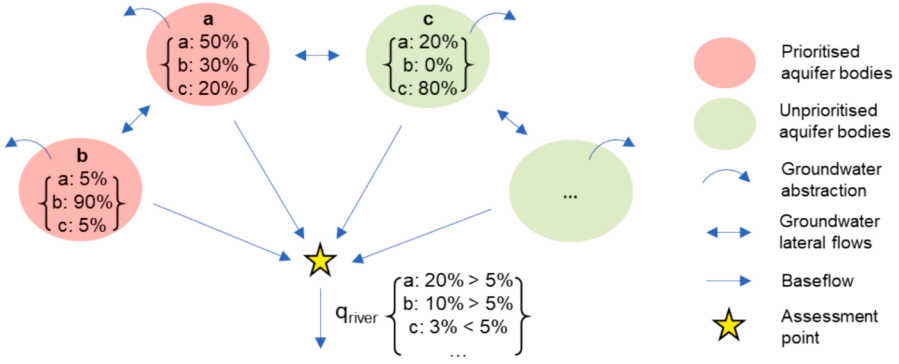

Strategies	Ratio of groundwater abstraction reduction			
	a	b	c	…
Equal-ratio	32%			
Prioritised	100%	100%	0%	0%
Prioritised and adjacent	50%+30%	5%+90%	20%+0%	…

Fig. 4. A conceptual example of strategies for groundwater abstraction reduction for river flow management at the assessment point.

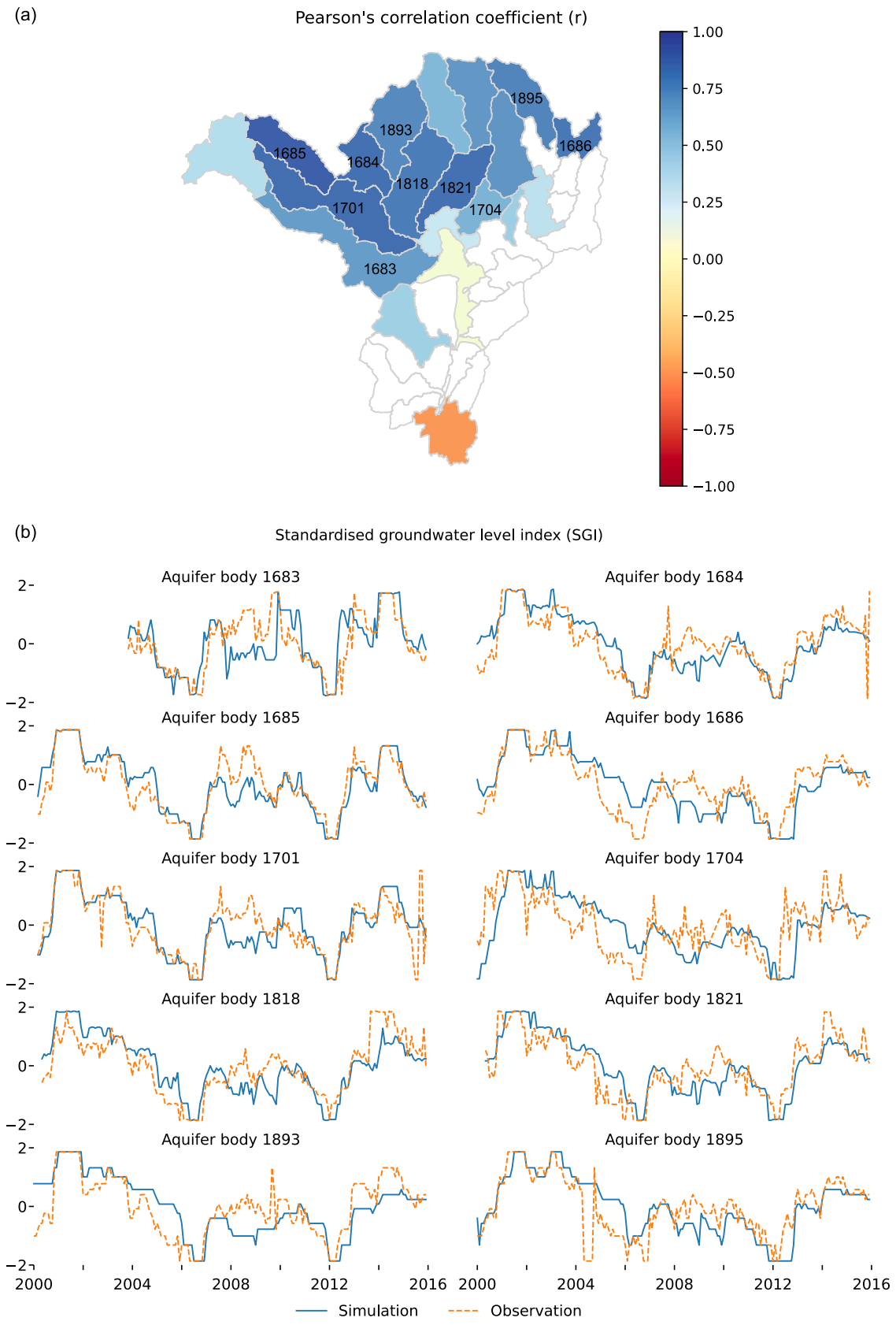

Fig. 5. Pearson's correlation coefficient (white sub-catchments denote no available observed groundwater levels) (a) and temporal comparison (b) of standardised groundwater level index (SGI) for monthly-averaged simulation and observation.

catchments have Pearson's correlation coefficient of more than 0.7, with time-series SGI matching well the observed data as shown in Fig. 5(b). Small discrepancies are observed between 2005–2010, when simulated SGI is higher before 2008 and lower after 2008 than the observed value, respectively (e.g., in the AB 1686 and 1893). This indicates that the droughts observed in these two periods are slightly under- and over-estimated, respectively, though the groundwater dynamics are simulated well overall.

The aquifer bodies in the middle region (AB 1897 and 1695), however, have correlation coefficients below 0.3, indicating a poor model performance. This result can be explained by the high number of abstraction boreholes concentrated in this area, which likely affects observed groundwater levels. Furthermore, the worst performance is observed at the lowest confined aquifer body (AB 1898), with a negative correlation observed. This is very likely to be caused by inaccurate model input of abstraction, which only has a constant value in this sub-

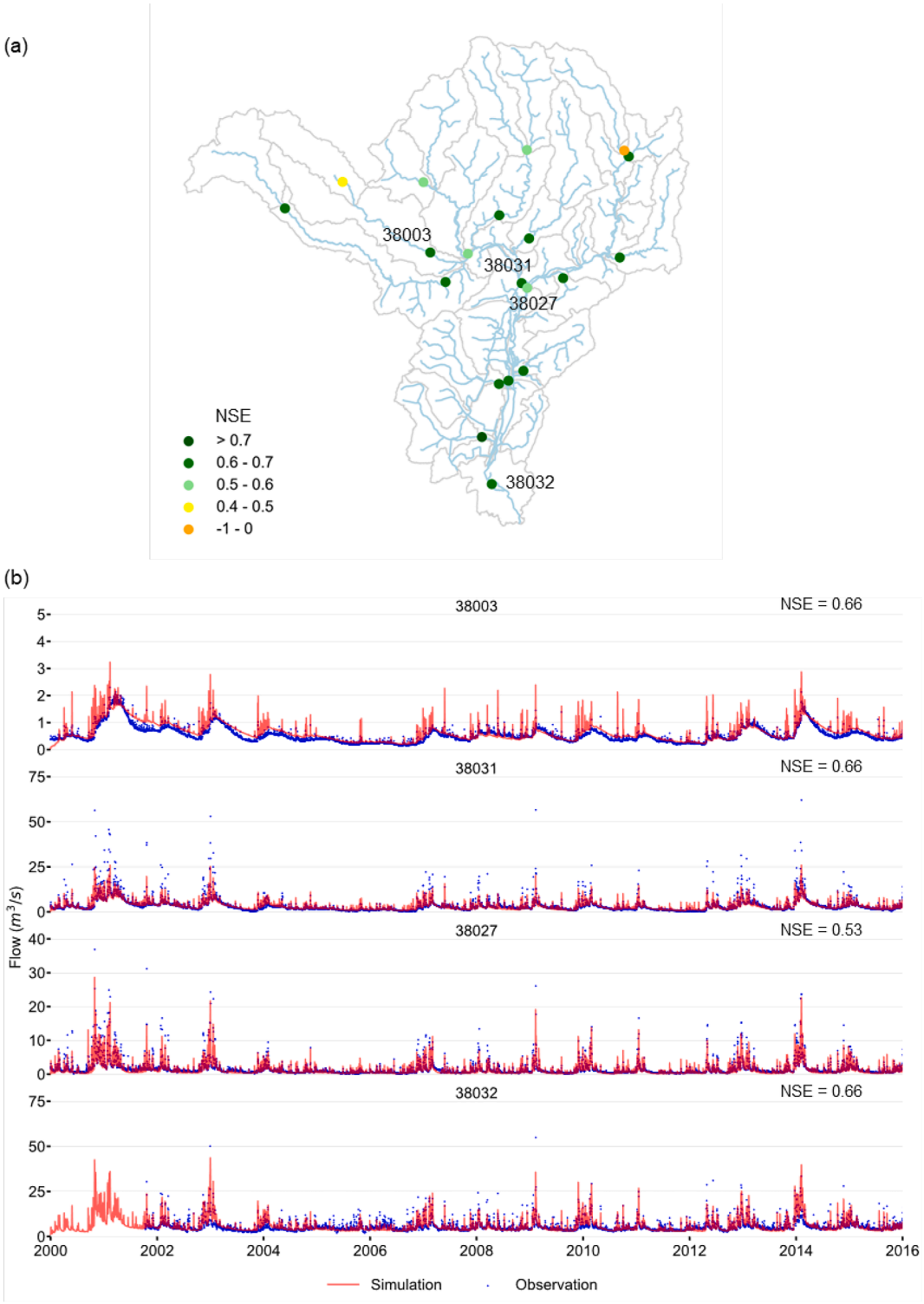

Fig. 6. Summary of Nash-Sutcliffe Efficiency (NSE) for river flow evaluation (a), with time series comparison of river flow against the observed data at the main tributaries from upstream to downstream (b). Contains Ordnance Survey data © Crown copyright and database right 2023.

catchment limited by data availability. The time-series comparison of these aquifer bodies can be seen in Fig. S1 in Supplementary Material.

Direct comparison of simulated and observed groundwater levels is difficult because modelled groundwater levels represent bulk groundwater storage over an aquifer body and observed levels are derived from measurements in boreholes at specific locations, the majority of which are nearby rivers, and thus controlled by the river stage. However, for completeness we present this comparison in Table S1 and Fig. S2 in Supplementary Material. For the absolute values of simulated and observed groundwater levels, 9 out of 20 aquifer bodies have mean absolute error (MAE) less than 10 m (Table S1). However, four aquifer bodies have MAE as large as around 30 m: the simulated groundwater levels in AB 1818 and 1821 are highly similar to the observations in two and one respective boreholes (around 50 mASL), with the remaining borehole having significantly low observations around 0 mASL in each aquifer body; in contrast, only one borehole is available for comparison in AB 1700 and 1897. Both instances demonstrate that the limited number of boreholes is not able to represent the average groundwater levels across these aquifer bodies and thus support the comparison. It is also noticed that the simulated average groundwater levels generally vary more significantly than the observed values (Fig. S2), which is due to the short distance of most boreholes to the rivers (Fig. 1(a)).

4.1.2. River flow

The Nash-Sutcliffe efficiency (NSE) results of simulated river flows against observations at the monitoring stations are summarised in Fig. 6 (a). 70 % (14 out of 20) stations have NSE above 0.6, and 90 % (18 out of 20) stations have NSE above 0.5, which demonstrates good simulation performance. The observed temporal patterns are successfully simulated and depicted at four stations on the main tributaries in Fig. 6(b), though some underestimations in high peaks are seen at Station 30031. Such underestimations are largely attributed to the smaller runoff generation, which can be caused by overestimated evapotranspiration and underestimated soil moisture content in the model, stemming from the accuracy for parameter evaluation (e.g., crop calendar, crop coefficient, and field capacity) using publicly available datasets. However, two stations have low NSE values (0.44 and −0.17), which are located at the north-east and north-west corners, respectively. This may be caused by inaccuracy in the model boundary conditions, which can have significant impacts on these two catchments' groundwater dynamics and consequently on baseflows to the rivers. The detailed metric values and time series comparison at all the stations are illustrated in the Supplementary Material.

4.2. Flux tracking

4.2.1. Origins of abstracted groundwater

The borehole abstraction predominantly comes from natural recharge, pipe leakage, and lateral flows entering the study area, tagged as 'Groundwater' (Fig. 7(a)). The minor proportion classified as 'Other' is observed in sub-catchment 1893, which comes from runoff through river leakage into the aquifer. However, the origins of the abstracted groundwater show significantly different patterns across the region. Water abstracted within some sub-catchments is virtually all allocated to the local aquifer body. These sub-catchments are mainly located at the upper boundaries, including 1823, 1683, 1684, 1896, 1686, and 1685. They have higher groundwater levels and are net exporters of water to adjacent aquifer bodies driven by the head gradient (Fig. S3 in Supplementary Material). As a result, the groundwater abstraction in the adjacent sub-catchments, including 1893, 1821, 1818, 1701, and 1820,

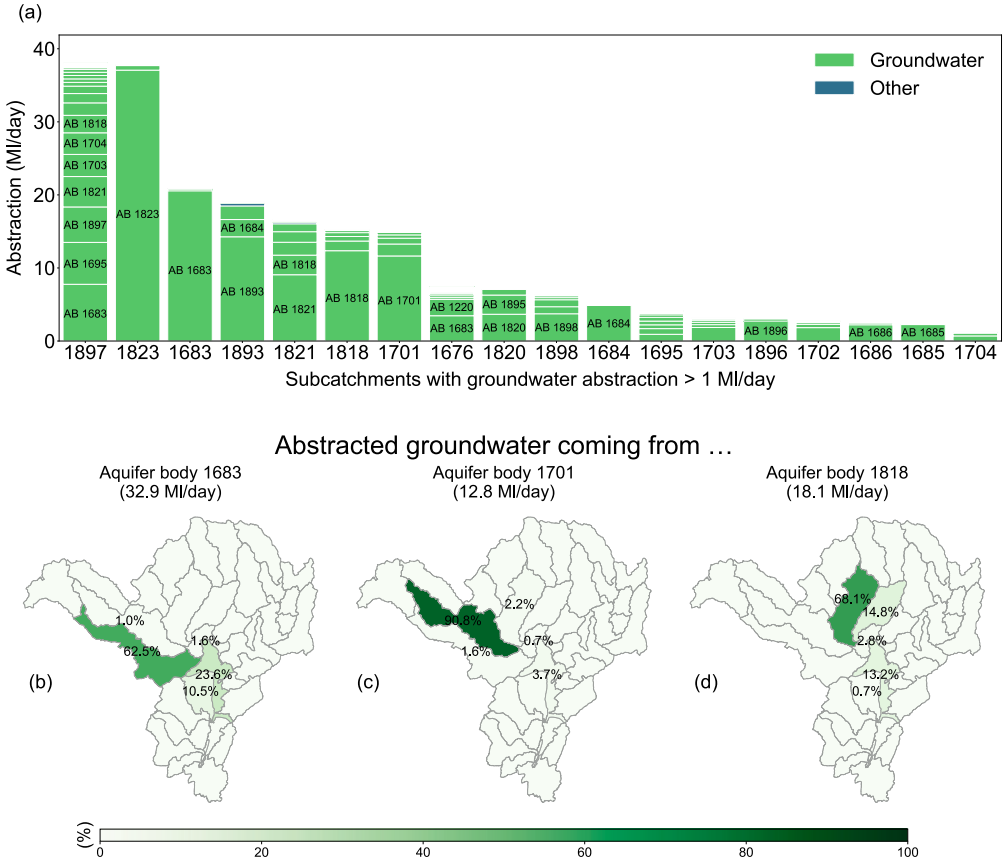

Fig. 7. Origins of abstracted water across the whole catchment in 2006–2015 (a), ordered from left to right based on the total amount of abstraction in each sub-catchment and ordered from bottom to top based on the proportions of water from different aquifer bodies (AB = Aquifer body); and the spatial distributions (b-d) of the abstracted water from the three prioritised aquifer bodies identified in Section 4.2.1.

contains water from the aquifer bodies in the upper areas, though the predominant proportion is still from local recharge. In contrast, the groundwater abstraction in sub-catchments 1897 and 1695 has diversified origins. In sub-catchment 1897, the predominant proportion is from the external aquifer bodies (AB 1683 and 1695), while the proportion of water from the local recharge is only ranked the third largest. This may imply that the significant amount of groundwater abstraction in AB 1897 (38 Ml/day averaged in 2006–2015) has created a cone of depression in the piezometric surface, which enlarged the head gradient between the middle area and the surrounding aquifer bodies and thus accelerated the groundwater lateral flows into the region.

The spatial distribution of abstracted groundwater originating from the three prioritised aquifer bodies (AB 1683, 1701, and 1818), which contribute the most to the baseflow at the assessment point (Section 4.2.1), is illustrated in Fig. 7(b-d). Among the three prioritised aquifer bodies, most water has been abstracted from AB 1683 (Fig. 7(b1)): 32.9 Ml/day, which is almost twice that from AB 1818 (18.1 Ml/day). The abstracted groundwater originating from these two aquifer bodies share a similar pattern of spatial distribution, with around two-thirds abstracted within the local sub-catchment (62.5 % and 68.1 %, respectively). The remaining one-third is abstracted from the adjacent sub-catchments: 23.8 % and 10.5 % within sub-catchments 1897 and 1676 for AB 1683, respectively; and 14.8 % and 13.2 % within sub-catchments 1821 and 1897 for AB 1818, respectively. In contrast, only 12.8 Ml/day abstracted groundwater originates from AB 1701, more than 90 % of which is abstracted within the local sub-catchment.

4.2.2. Origins of river flow at the assessment point

The time series of flux tracking results identifies the origins of river flows at the assessment point between 2006 and 2015 (Fig. 8(a)). A significant seasonal variation can be observed, with baseflow ('Groundwater' in the figure) accounting for higher percentages of daily river flows in the dry season (55 % on average from May to August) than wet season (31 % on average from November to February). In the wet season, the dominant proportion of river flow is tagged as 'Other', which comes from surface and subsurface runoff and urban stormwater. However, the pattern was different in an abnormally wet year in 2012, when runoff and stormwater dominated. Such seasonal variations of the composition of river flow are consistent with the previous integrated modelling by Liu et al. (2023) in the other UK catchments. Specifically in the dry season, the groundwater contributed to almost half (47 %) of the river flow in total from 2006 to 2015 (Fig. 8(b)), with the other half coming from wastewater effluent and urban stormwater. Among the baseflow fluxes, AB 1683, 1701, and 1818 account for the largest proportions, with 19 %, 13 %, and 5 %, respectively. These aquifer bodies are located in the north-west of the catchment (Fig. 8(c)), where reductions in groundwater abstraction should be prioritised for baseflow improvement. The contributions from the rest of the aquifer bodies are small (mostly < 1 %).

4.3. Strategy performance

4.3.1. Abstraction reduction

Strategies designed with and without knowing the origins of water fluxes have different spatial distributions of groundwater abstraction reduction. Without the insights, a 32 % equal reduction results in an approximately 13 Ml/day decrease in sub-catchments 1897 and 1823, with < 7 Ml/day in the rest (Fig. 9(a)). After knowing that AB 1683, 1701, and 1818 contribute to the largest proportions of baseflow at the assessment point, the abstraction is fully reduced by around 19 Ml/day in AB 1683 and by 15 Ml/day in the other two aquifer bodies, respectively (Fig. 9(b)). To further protect water resources in the prioritised aquifer bodies (Fig. 9(c)), sub-catchment 1897 reduces abstraction by around 11 Ml/day, and sub-catchments 1676, 1821, and 1695 reduce abstraction by less than 4 Ml/day, respectively, because they all have various degrees of access via groundwater lateral flows (Fig. 7(b-d)).

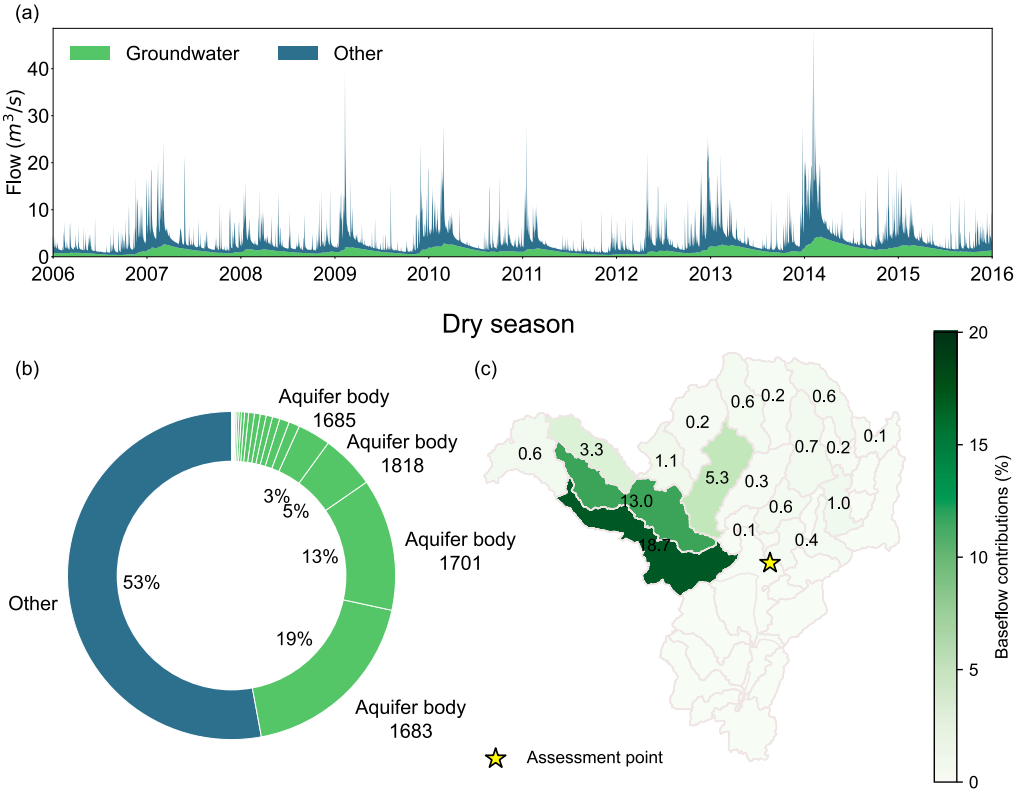

Fig. 8. Timeseries illustration of river flow origins at the assessment point in 2006–2015 (a) and the detailed proportions in the dry season (b), with the spatial distribution of baseflow contributions (c).

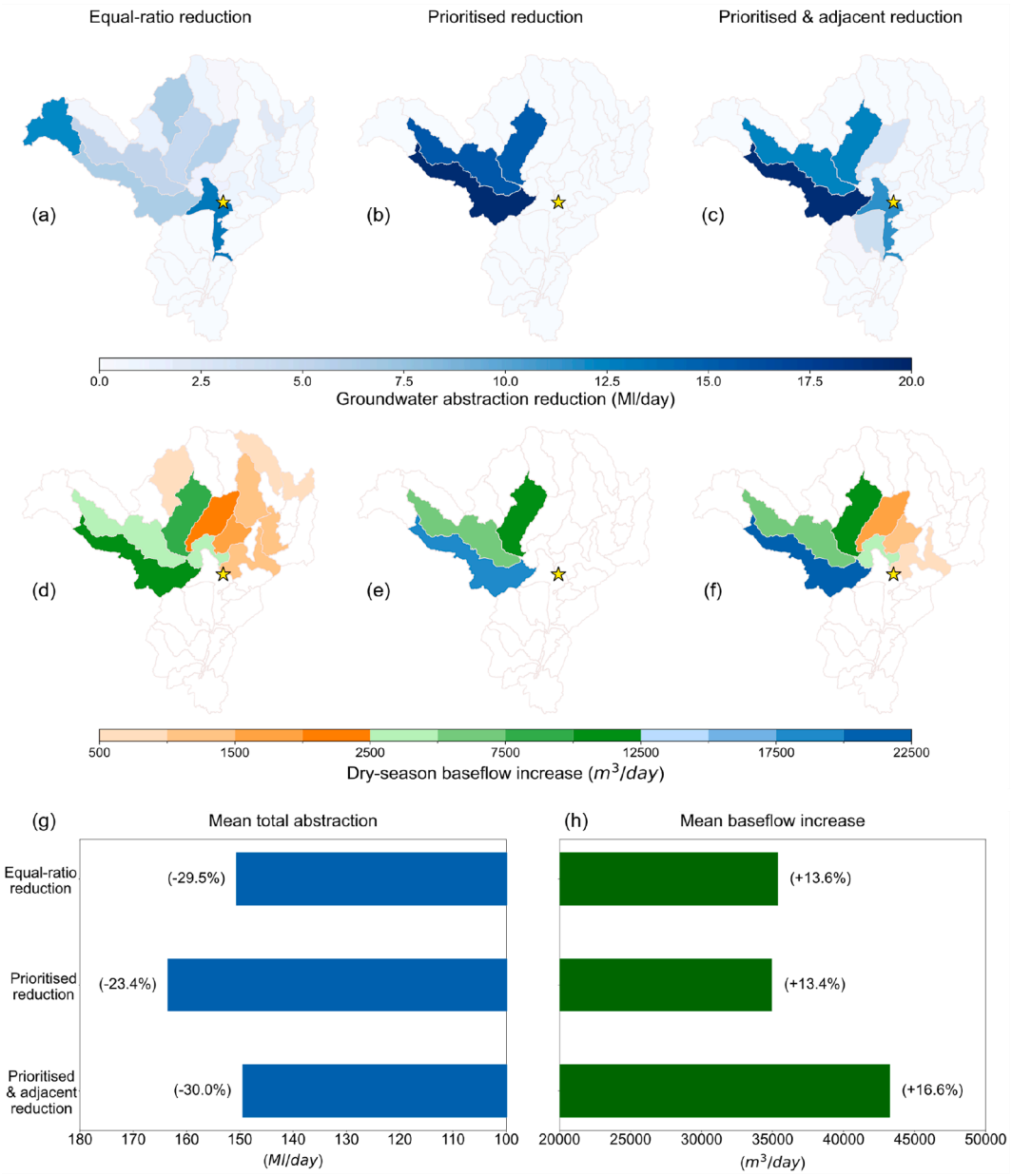

Fig. 9. Spatial distribution of groundwater abstraction reduction (a-c) and mean baseflow increase in dry seasons during the simulation period in the three scenarios (d-f). Their performance in mean total abstraction within the whole catchment (g) and mean baseflow increase at the assessment point (labelled as yellow stars) (h) are summarised as well (numbers in brackets are the relative change compared to the baseline scenario). (For interpretation of the references to colour in this figure legend, the reader is referred to the web version of this article.)

4.3.2. *Baseflow increase*

The three strategies have different impacts on baseflow to the rivers upstream of the assessment point (Fig. 9(d-f)). The equal reduction strategy produces a minor increase in baseflow (<2,500 m^3/day) in most sub-catchments, with the highest increase in sub-catchments 1683 and 1818 (~10,000 m^3/day). The prioritised reduction strategy has more baseflow increase in these sub-catchments, especially in sub-catchment 1683 where a nearly 20,000 m^3/day increase is simulated. However, the rest of the sub-catchments have virtually no increase in baseflow due to no change in abstraction. In comparison, the last strategy mildly increases baseflows by less than 3,000 m^3/day in sub-catchments 1695, 1821, and 1704, because abstraction reduction in these sub-catchments increased the groundwater level. Moreover, the increased groundwater level in sub-catchment 1897 reduces the regional head gradient between aquifer bodies, so that less lateral flow leaves AB 1683. This consequently increases the groundwater level in AB 1683 and leads to the most substantial baseflow increase (>22,000 m^3/day) of all the strategies.

4.3.3. *System-level performance*

As for the overall systems performance (Fig. 9(g-h)), the mean total groundwater abstraction is reduced by 29.5 % in the equal-ratio reduction strategy, with 151 Ml/day. Such a reduction increases the dry season river flow by 13.6 % at the assessment point, with 35,369 m^3/day. A similar baseflow increase is obtained by the prioritised reduction strategy, which, however, only reduces the mean total abstraction by 23.4 %. The mean total groundwater abstraction after reduction is 164 Ml/day, which is 13 Ml/day higher than the equal-ratio reduction strategy. Finally, the 'prioritised and adjacent reduction' strategy increases the baseflow by the largest percentage (16.4 %), which is nearly 10,000 m^3/day more than the other two strategies. This increase, however, is achieved by reducing a similar amount of

abstraction (30.3 %) with the equal-ratio reduction strategy. Overall, both strategies obtain better performance than the equal reduction by more efficiently improving the baseflow.

5. Discussion

5.1. Groundwater modelling within integrated water systems

The first contribution of this study has been to develop a reduced-complexity, process-based groundwater module within an integrated modelling framework (WSIMOD-GW). Through evaluation against observed data, the model can largely capture the dynamics of surface and groundwater in the system. WSIMOD-GW can simulate not only groundwater levels and head-driven lateral flows that are normally not physically represented by the catchment hydrological models but also the interactions between groundwater and the other natural and built components in the integrated water cycle flexibly. The reduced-complexity model structure limits the computational demand and makes this model very suitable for designing and testing groundwater management strategies and evaluating their performance at a systems level.

Compared to the parsimonious groundwater representations in the default WSIMOD, the introduced parameters (e.g., riverbed conductance) and variables (e.g., lateral groundwater flows) increase the uncertainties in the model, though most of the parameters have a physical meaning. To constrain the uncertainties, the aquifer conductance and lateral flows crossing the outer boundaries are acquired from the existing distributed groundwater national-scale numerical model, BGWM, developed by the BGS (Bianchi et al., 2024), and only riverbed conductance is manually calibrated for baseflow simulation. However, the current national-scale model may not be able to reveal the detailed local dynamics accurately. This may be particularly significant at the boundary of aquifer bodies which are directly impacted by the specified lateral fluxes, evidenced by the sub-catchment 1685 and 1895 having poor NSE in river flow. In the strategy testing, decreasing groundwater abstraction at the boundary sub-catchments may impact external lateral groundwater flows in reality, which introduces errors in the boundary conditions. The study area could be expanded to include buffer regions so that internal groundwater abstraction cannot significantly impact the boundary lateral flows, but this would require additional model input data. Alternatively, the need to derive specified boundary fluxes from the BGWM could be removed by defining Cauchy-type head-dependent boundary fluxes but these would likely require model calibration. To be fully decoupled from BGWM, the aquifer conductance in WSIMOD-GW could be derived from transmissivity data (Griffiths et al., 2023). Point transmissivity data from the database of Allen et al. (1997) could be used to infer reasonable estimates at sub-catchment scales. However, the calibrated transmissivity 'map' from the BGWM, or from the set of regional groundwater models that have been developed in the UK (Whiteman et al., 2012) (if they were collated into a contiguous dataset) could be used as stand-alone model input datasets. Though additional work is needed to improve the derivation of a spatial groundwater level map, based on point groundwater level observations, such a dataset does exist (McKenzie, 2015), which could be used to constrain WSIMOD parameterisation and evaluation.

5.2. System diagnosis via flux tracking

As the second contribution, this study developed a flux tracking approach that reveals the origins of water fluxes as a systems diagnosis. The results illustrate the temporal variation and spatial distribution of river flow origins at an assessment point, providing insights into identifying aquifer bodies that have significant contributions to baseflow and should be prioritised for regulation. Compared to the baseflow index (BFI) derived based on the river hydrograph, this approach has the advantage of distinguishing between groundwater and wastewater effluent. This is particularly important in urbanised catchments where the rivers receive significant quantities of effluent (e.g., ~40 Ml/day simulated in the Upper Lea catchment). This proportion has often been accounted as baseflow in BFI, and the groundwater contribution to the dry season river flow tends to be overestimated, which can be avoided by flux tracking.

The results also show the origins of groundwater abstracted in different sub-catchments: in some sub-catchments (e.g., 1701) abstracted groundwater mostly comes from local recharge, while in other sub-catchments (e.g., 1897) abstracted groundwater originates from a diverse set of aquifer bodies. This stimulates the strategy design to consider the impacts of groundwater abstraction not only on local sub-catchments but also on external aquifer bodies through lateral flows. To further evaluate such impacts at boundary aquifer bodies, the lateral flows into the study area, which are currently tagged using the receiving aquifer body's name, should be further delineated and tracked. This is particularly important in those aquifer bodies that have received significant quantities (e.g., nearly 40,000 m^3/day on average into AB 1683 from outside the domain).

As the key hypothesis of the flux tracking, complete mixing is assumed in the aquifer bodies, which generates identical flux compositions in all the outflows, including baseflow to rivers, groundwater lateral flows, and abstraction (Fig. 3). However, this might not reflect the reality, evidenced by the stratified vertical water age distributions in previous studies (Ayraud et al., 2008). Shallow layers having younger water directly interact with recharge and rivers, while groundwater in deeper layers will be older. This implies that a vertical distribution of water from different origins may also exist, which may generate different compositions of fluxes in the outflows. Recharge tagged with the local aquifer body's name at the upper layer contributes more to the baseflow, while groundwater through lateral flows residing at the lower layer is more often accessed by pumped boreholes. As a result, the composition of the outflows may significantly differ from this study's results, especially in those aquifer bodies containing water from diverse origins (e.g., AB 1897 in Fig. 7(a)). To reveal such a vertical distribution and enable more accurate flux tracking, the groundwater module in this study can be further developed into a multi-layer configuration to represent the vertical subsurface processes. Furthermore, the flux tracking approach based on conceptual modelling could be validated by particle tracking using numeric models in theory. This might mean specifying many classes of tracers to represent water from various sources entering individual aquifer bodies, inducing significant computational demand.

5.3. Better systems performance via integrated water resources management

Based on the flux tracking insights, the third contribution in this study has been to test groundwater abstraction reduction strategies that can more efficiently improve baseflow at the assessment point. Simulations show that targeting the reductions to the aquifer bodies that contribute the most to river baseflow can result in an increment in baseflow comparable to a uniform reduction, but with a higher efficiency by preserving more total groundwater abstraction. On this basis, reducing abstraction further in the adjacent sub-catchments can preserve more water within these aquifer bodies by reducing the groundwater lateral flows, which generates more baseflows to the downstream assessment point. Both strategies are demonstrated to obtain better system performance and help to manage the conflicts between water use and baseflow maintenance. This highlights the need to obtain deep insights via a holistic diagnosis in the integrated water system to inform the management of groundwater resources.

The results show that a 30 % mean total abstraction reduction can improve the mean dry season baseflow at the assessment point by around 16 %. This demonstrates that only relying on groundwater abstraction reduction for baseflow improvement may not be sufficient. It

is necessary to manage the 'Other' fluxes in the dry season, which account for more than half of the river flow (Fig. 8(b)). The 'Other' fluxes should be further delineated based on their specific origins, including surface and subsurface runoff, storm and wastewater flows, etc., which requires the implementation of this flux tracking approach with integrated modelling. This could enable a full systems diagnosis to coordinate the management of different components (e.g., surface water abstraction and groundwater abstraction) for better performance. It is also noted that both strategies concentrate abstraction reduction into several catchments (Fig. 9(b-c)), which might significantly interfere with the local water supply and water use activities. To assess the potential impacts as well as prevent unintended consequences, more management objectives representing stakeholders' interests should be incorporated in the strategy design and evaluation, among which the trade-offs should be revealed by techniques such as multi-objective optimisation (Liu et al., 2023b) and multi-criteria analysis (Calizaya et al., 2010).

6. Conclusions

To understand the role of groundwater in integrated water resources management, this study developed a reduced-complexity, process-based groundwater module and incorporated it into the water systems integration model (WSIMOD-GW). To show the ability of the model to simulate all the components of the water budget, the model was applied to a complex catchment system in the UK. The model shows good performance in capturing the spatio-temporal dynamics in groundwater levels and river flows and is thus suitable for systems analysis.

To quantify groundwater interactions with other components in the water system, a flux tracking approach was developed, which characterises the origins of fluxes in the river and abstracted groundwater. Through the case study, this approach identified the dominant contributing aquifer bodies to the dry season river flow at an assessment point and revealed the spatial distributions of the abstracted groundwater originating from them. The information was used to design two groundwater abstraction reduction strategies. Both strategies were demonstrated to more efficiently improve the dry season baseflow at the assessment point than the one without flux tracking information.

Overall, WSIMOD-GW is a useful tool for investigating groundwater interactions and exploring systems complexity to inform large-scale integrated water resources management, which complements the use of numeric models for understanding detailed subsurface processes and hydrogeological heterogeneity. Future work could compare the simulation performance of the groundwater models across varying degrees of complexities for elaborating their strengths and weakness to better guide model use. Wider model application would benefit from improvements to, or the creation of openly available, spatially contiguous data on aquifer properties and groundwater levels. This would remove the dependence of WSIMOD-GW on information from the distributed national groundwater model, though BGWM's parameterisation could be used to generate these open datasets. The generic flux tracking approach can be applied to any water fluxes in the system for a more holistic systems diagnosis. This enables the coordination of management measures that intervene in different fluxes and obtain better systems-level performance that could satisfy multiple stakeholders' interests.

CRediT authorship contribution statement

Leyang Liu: Writing – review & editing, Writing – original draft, Visualization, Validation, Software, Methodology, Investigation, Formal analysis. **Marco Bianchi:** Writing – review & editing, Resources, Methodology, Investigation, Data curation, Conceptualization. **Christopher R. Jackson:** Writing – review & editing, Visualization, Supervision, Resources, Project administration, Methodology, Conceptualization. **Ana Mijic:** Writing – review & editing, Supervision, Resources, Project administration, Funding acquisition.

Declaration of competing interest

The authors declare that they have no known competing financial interests or personal relationships that could have appeared to influence the work reported in this paper.

Data availability

This study uses both publicly avaiable and licensed data, the former of which will be made available on request.

Acknowledgements

The research reported in this paper was undertaken as part of the CAMELLIA (Community Water Management for a Liveable London) project, funded by the Natural Environment Research Council (NERC) under grant NE/S003495/1. Bianchi and Jackson publish with the permission of the Executive Director of the British Geological Survey. The authors are grateful to Dr. Ilias Karapanos, Affinity Water, for comments on the manuscript that have improved the paper.

Appendix A. Supplementary data

Supplementary data to this article can be found online at https://doi.org/10.1016/j.jhydrol.2024.131379.

References

Affinity Water. 2022. *Deployable Output Benefits from Abstraction Reduction: Technical Appendix.*

Environment Agency. (2020) *CAMS: London abstraction licensing strategy* .

Allen, D. J., Brewerton, L. J., Coleby, L. M., Gibbs, B. R., Lewis, M. A., MacDonald, A. M., Wagstaff, S. J., Williams, A. T. 1997. The physical properties of major aquifers in England and Wales.

Anderson, M. P., Woessner, W. W., Hunt, R. J. 2015. *Applied Groundwater Modeling: Simulation of Flow and Advective Transport. [google]* Academic Press.

Ayraud, V., Aquilina, L., Labasque, T., Pauwels, H., Molenat, J., Pierson-Wickmann, A., Durand, V., Bour, O., Tarits, C., Le Corre, P., 2008. Compartmentalization of physical and chemical properties in hard-rock aquifers deduced from chemical and groundwater age analyses. Appl. Geochem. 23 (9), 2686–2707.

Baalousha, H.M., 2012. Characterisation of groundwater–surface water interaction using field measurements and numerical modelling: a case study from the Ruataniwha Basin, Hawke's Bay, New Zealand. *Appl. Water Sci.* 2 (2), 109–118.

Barrett, M.E., Charbeneau, R.J., 1997. A parsimonious model for simulating flow in a karst aquifer. J. Hydrol. 196 (1–4), 47–65.

Barthel, R., 2006. Common problematic aspects of coupling hydrological models with groundwater flow models on the river catchment scale. Adv. Geosci. 9, 63–71.

Bergström, S., Lindström, G., 2015. Interpretation of runoff processes in hydrological modelling—experience from the HBV approach. Hydrol. Process. 29 (16), 3535–3545.

Bianchi, M., Scheidegger, J.M., Hughes, A.G., Jackson, C.R., Lee, J.R., Lewis, M.A., Mansour, M., Newell, A.J., Dochartaigh, O.B., Patton, A.M., Dadson, S.J., 2024. Simulation of national-scale groundwater dynamics in geologically complex aquifer systems: an example from Great Britain. Hydrol. Sci. J. 69 (5), 572–591.

Bloomfield, J.P., Marchant, B.P., 2013. Analysis of groundwater drought building on the standardised precipitation index approach. Hydrol. Earth Syst. Sci. 17 (12), 4769–4787.

Botter, G., Bertuzzo, E., Rinaldo, A., 2010. Transport in the hydrologic response: Travel time distributions, soil moisture dynamics, and the old water paradox. Water Resour. Res. 46 (3).

Brunner, P., Therrien, R., Renard, P., Simmons, C.T., Franssen, H.H., 2017. Advances in understanding river-groundwater interactions. Rev. Geophys. 55 (3), 818–854.

Calizaya, A., Meixner, O., Bengtsson, L., Berndtsson, R., 2010. Multi-criteria decision analysis (MCDA) for integrated water resources management (IWRM) in the Lake Poopo Basin, Bolivia. Water Resour. Manage. 24 (10), 2267–2289.

Camporese, M., Paniconi, C., Putti, M., Orlandini, S., 2010. Surface-subsurface flow modeling with path-based runoff routing, boundary condition-based coupling, and assimilation of multisource observation data. Water Resour. Res. 46 (2).

Chen, X., Yin, Y., 2001. Streamflow depletion: Modeling of reduced baseflow and induced stream infiltration from seasonally pumped wells. J. Am. Water Resour. Assoc. 37 (1), 185–195.

Department for Environment Food & Rural Affairs. 2023. *Hydrology Data Explorer.* https://environment.data.gov.uk/hydrology/explore.

Department for Environment, Food and Rural Affairs. 2019. *Abstraction Reform Report - Progress Made in Reforming the Arrangements Formanaging Water Abstraction in England.*

Department for Environment, Food and Rural Affairs. 2021. *Water Abstraction Plan: Environment.*
Diersch, H.G., 2013. FEFLOW: Finite Element Modeling of Flow, Mass and Heat Transport in Porous and Fractured Media. [google] Springer Science & Business Media.
Dobson, B., Mijic, A., 2020. Protecting rivers by integrating supply-wastewater infrastructure planning and coordinating operational decisions. Environ. Res. Lett. 15 (11), 114025.
Dobson, B., Jovanovic, T., Chen, Y., Paschalis, A., Butler, A., Mijic, A., 2021. Integrated Modelling to support analysis of COVID-19 impacts on London's water system and in-river water quality. Front. Water 3, 641462. https://doi.org/10.3389/Frwa.
Dobson, B., Liu, L., Mijic, A., 2023. Water Systems Integrated Modelling framework, WSIMOD: A Python package for integrated modelling of water quality and quantity across the water cycle. J. Open Source Softw. 8 (83), 4996.
Dobson, B. 2022. *WSIMOD Documentation.* https://imperialcollegelondon.github.io/wsi/.
Eberts, S.M., Böhlke, J.K., Kauffman, L.J., Jurgens, B.C., 2012. Comparison of particle-tracking and lumped-parameter age-distribution models for evaluating vulnerability of production wells to contamination. Hydrgeol. J. 20 (2), 263.
Environment Agency. 2019. *Till Abstraction Licensing Strategy.*
Environment Agency. 2021. *WFD River Waterbody Catchments Cycle 2.* https://data.gov.uk/dataset/298258ee-c4a0-4505-a3b5-0e6585ecfdb2/wfd-river-waterbody-catchments-cycle-2.
Environment Agency. 2023. *LIDAR Composite DTM 2022 – 10m.* https://www.data.gov.uk/dataset/7f31af0f-bc98-4761-b4b4-147bfb986648/lidar-composite-dtm-2022-10m.
Ewen, J., Parkin, G., O'Connell, P.E., 2000. SHETRAN: Distributed river basin flow and transport modeling system. J. Hydrol. Eng. 5 (3), 250–258.
Flynn, N.J., Paddison, T., Whitehead, P.G., 2002. INCA Modelling of the Lee System: strategies for the reduction of nitrogen loads. Hydrol. Earth Syst. Sci. 6 (3), 467–484.
Gaiser, T., Printz, A., von Raumer, H.S., Götzinger, J., Dukhovny, V.A., Barthel, R., Sorokin, A., Tuchin, A., Kiourtsidis, C., Ganoulis, I., 2008. Development of a regional model for integrated management of water resources at the basin scale. Phys. Chem. Earth, Parts A/B/C 33 (1–2), 175–182.
Gao, H., Tang, Q., Shi, X., Zhu, C., Bohn, T., Su, F., Pan, M., Sheffield, J., Lettenmaier, D., Wood, E. 2010. Water budget record from Variable Infiltration Capacity (VIC) model.
Griffiths, J., Yang, J., Woods, R., Zammit, C., Porhemmat, R., Shankar, U., Rajanayaka, C., Ren, J., Howden, N., 2023. Parameterization of a National Groundwater Model for New Zealand. Sustainability. 15 (17), 13280.
Guillaumot, L., Smilovic, M., Burek, P., De Bruijn, J., Greve, P., Kahil, T., Wada, Y., 2022. Coupling a large-scale hydrological model (CWatM v1. 1) with a high-resolution groundwater flow model (MODFLOW 6) to assess the impact of irrigation at regional scale. Geosci. Model Dev. 15 (18), 7099–7120.
Gusyev, M.A., Abrams, D., Toews, M.W., Morgenstern, U., Stewart, M.K., 2014. A comparison of particle-tracking and solute transport methods for simulation of tritium concentrations and groundwater transit times in river water. Hydrol. Earth Syst. Sci. 18 (8), 3109–3119.
Haque, A., Salama, A., Lo, K., Wu, P., 2021. Surface and groundwater interactions: a review of coupling strategies in detailed domain models. Hydrology 8 (1), 35.
Harries, J.E., Sheahan, D.A., Matthiessen, P., Neall, P., Rycroft, R., Tylor, T., Jobling, S., Routledge, E.J., Sumpter, J.P., 1996. A survey of estrogenic activity in United Kingdom inland waters. Environ. Toxicol. Chem. 15 (11), 1993–2002.
Hill, M. C., Banta, E. R., Harbaugh, A. W., Anderman, E. R. 2000. *MODFLOW-2000, the US Geological Survey Modular Ground-Water Model; User Guide to the Observation, Sensitivity, and Parameter-Estimation Processes and Three Post-Processing Programs.* US Geological Survey.
Hrachowitz, M., Savenije, H., Bogaard, T.A., Tetzlaff, D., Soulsby, C., 2013. What can flux tracking teach us about water age distribution patterns and their temporal dynamics? Hydrol. Earth Syst. Sci. 17 (2), 533–564.
Hughes, D.A., Kapangaziwiri, E., Baker, K., 2010. Initial evaluation of a simple coupled surface and ground water hydrological model to assess sustainable ground water abstractions at the regional scale. Hydrol. Res. 41 (1), 1–12.
HYPE Model Documentation. 2021. *HYPE model description.* [Accessed 2021].
Ivkovic, K. M., 2006. Modelling groundwater-river interactions for assessing water allocation options.
Jing, M., Heße, F., Kumar, R., Wang, W., Fischer, T., Walther, M., Zink, M., Zech, A., Samaniego, L., Kolditz, O. 2018. Improved regional-scale groundwater representation by the coupling of the mesoscale Hydrologic Model (mHM v5. 7) to the groundwater model OpenGeoSys (OGS). *Geosci. Model Develop.* 11 (5), 1989-2007.
Jing, M., Kumar, R., Attinger, S., Li, Q., Lu, C., Hesse, F., 2021. Assessing the contribution of groundwater to catchment travel time distributions through integrating conceptual flux tracking with explicit Lagrangian particle tracking. Adv. Water Resour. 149, 103849.
Jukić, D., Denić-Jukić, V., 2009. Groundwater balance estimation in karst by using a conceptual rainfall–runoff model. J. Hydrol. 373 (3–4), 302–315.
Kaandorp, V., De Louw, P., Van der Velde, Y., Broers, H.P., 2018. Transient groundwater travel time distributions and age-ranked storage-discharge relationships of three lowland catchments. Water Resour. Res. 54 (7), 4519–4536.
Kaandorp, V., Broers, H.P., Van Der Velde, Y., Rozemeijer, J., De Louw, P.G., 2021. Time lags of nitrate, chloride, and tritium in streams assessed by dynamic groundwater flow tracking in a lowland landscape. Hydrol. Earth Syst. Sci. 25 (6), 3691–3711.
Kim, N.W., Chung, I.M., Won, Y.S., Arnold, J.G., 2008. Development and application of the integrated SWAT–MODFLOW model. J. Hydrol. 356 (1–2), 1–16.
Kirchner, J.W., 2016. Aggregation in environmental systems–Part 2: Catchment mean transit times and young water fractions under hydrologic nonstationarity. Hydrol. Earth Syst. Sci. 20 (1), 299–328.
Knoben, W., 2019. Investigating Conceptual Model Structure Uncertainty: Progress in Large-Sample Comparative Hydrology. University of Bristol.
Knox, J., Haro, D., Hess, T., 2017. *Task 2 Agricultural Water Demand Forecasts: Baseline Demand (Part I).*
Kollet, S.J., Maxwell, R.M., 2006. Integrated surface–groundwater flow modeling: A free-surface overland flow boundary condition in a parallel groundwater flow model. Adv. Water Resour. 29 (7), 945–958.
Kumar, R., Heße, F., Rao, P., Musolff, A., Jawitz, J.W., Sarrazin, F., Samaniego, L., Fleckenstein, J.H., Rakovec, O., Thober, S., 2020. Strong hydroclimatic controls on vulnerability to subsurface nitrate contamination across Europe. Nat. Commun. 11 (1), 6302.
Lancia, M., Petitta, M., Zheng, C., Saroli, M., 2020. Hydrogeological insights and modelling for sustainable use of a stressed carbonate aquifer in the Mediterranean area: From passive withdrawals to active management. J. Hydrol.: Reg. Stud. 32, 100749.
Lapworth, D.J., Dochartaigh, B.Ó., Nair, T., O'Keeffe, J., Krishan, G., MacDonald, A.M., Khan, M., Kelkar, N., Choudhary, S., Krishnaswamy, J., 2021. Characterising groundwater-surface water connectivity in the lower Gandak catchment, a barrage regulated biodiversity hotspot in the mid-Gangetic basin. J. Hydrol. 594, 125923.
Li, X., Cheng, G., Ge, Y., Li, H., Han, F., Hu, X., Tian, W., Tian, Y., Pan, X., Nian, Y., 2018. Hydrological cycle in the Heihe River Basin and its implication for water resource management in endorheic basins. J. Geophys. Res. Atmos. 123 (2), 890–914.
Liu, L., Dobson, B., Mijic, A., 2021. Hierarchical systems integration for coordinated urban-rural water quality management at a catchment scale. Sci. Total Environ., 150642
Liu, L., Dobson, B., Mijic, A., 2023a. Water quality management at a critical checkpoint by coordinated multi-catchment urban-rural load allocation. J. Environ. Manage. 340, 117979.
Liu, L., Dobson, B., Mijic, A., 2023b. Optimisation of Urban-Rural Nature-Based Solutions for Integrated Catchment Water Management.J. Environ. Manage. 329, 117045.
Ma, L., He, C., Bian, H., Sheng, L., 2016. MIKE SHE modeling of ecohydrological processes: Merits, applications, and challenges. Ecol. Eng. 96, 137–149.
Mackay, J.D., Jackson, C.R., Wang, L., 2014. A lumped conceptual model to simulate groundwater level time-series. Environ. Model. Softw. 61, 229–245.
Marsh, T. J., Cole, G. A. 2006. A review of the GLA drought severity assessments presented at the Beckton Gateway WTW Public Enquiry.
Marsili, A., Karapanos, I., Jaweesh, M., Yarker, D.R., Powers, E.M., Sage, R.C., 2023. Artesian conditions in the Chilterns Chalk aquifer (NW of the London Basin) and the implications for surface water–groundwater interactions. Geol. Soc. Lond. Spec. Publ. 517 (1), SP517-144.
McDonnell, J.J., McGuire, K., Aggarwal, P., Beven, K.J., Biondi, D., Destouni, G., Dunn, S., James, A., Kirchner, J., Kraft, P., 2010. How old is streamwater? Open questions in catchment transit time conceptualization, modelling and analysis. Hydrol. Process. 24 (12), 1745–1754.
McKenzie, A. A., 2015. User guide for the British Geological Survey National Depth to Groundwater Dataset.
Moriasi, D.N., Arnold, J.G., Van Liew, M.W., Bingner, R.L., Harmel, R.D., Veith, T.L., 2007. Model evaluation guidelines for systematic quantification of accuracy in watershed simulations. Trans. ASABE 50 (3), 885–900.
Morton, D., Marston, C., O'Neil, A., Rowland, C. 2022. Land Cover Map 2019 (1km summary rasters, GB and N. Ireland). *NERC EDS Environmental Information Data Centre.* https://doi.org/10.5285/e5632f1b-040c-4c39-8721-4834ada6046a.
Neitsch, S.L., Arnold, J.G., Kiniry, J.R., Williams, J.R., 2011. Soil and Water Assessment Tool Theoretical Documentation Version 2009. Texas Water Resources Institute.
Oldham, L.D., Freer, J., Coxon, G., Howden, N., Bloomfield, J.P., Jackson, C., 2023. Evidence-based requirements for perceptualising intercatchment groundwater flow in hydrological models. Hydrol. Earth Syst. Sci. 27 (3), 761–781.
Perrin, C., Michel, C., Andréassian, V., 2003. Improvement of a parsimonious model for streamflow simulation. J. Hydrol. 279 (1–4), 275–289.
Prucha, B., Graham, D., Watson, M., Avenant, M., Esterhuyse, S., Joubert, A., Kemp, M., King, J., le Roux, P., Redelinghuys, N., 2016. MIKE-SHE integrated groundwater and surface water model used to simulate scenario hydrology for input to DRIFT-ARID: The Mokolo River case study. Water SA 42 (3), 384–398.
Remondi, F., Kirchner, J.W., Burlando, P., Fatichi, S., 2018. Water flux tracking with a distributed hydrological model to quantify controls on the spatio-temporal variability of transit time distributions. Water Resour. Res. 54 (4), 3081–3099.
Rinaldo, A., Beven, K.J., Bertuzzo, E., Nicotina, L., Davies, J., Fiori, A., Russo, D., Botter, G., 2011. Catchment travel time distributions and water flow in soils. Water Resour. Res. 47 (7).
Samaniego, L., Kumar, R., Jackisch, C., 2011. Predictions in a data-sparse region using a regionalized grid-based hydrologic model driven by remotely sensed data. Hydrol. Res. 42 (5), 338–355.
Scheidegger, J.M., Jackson, C.R., Muddu, S., Tomer, S.K., Filgueira, R., 2021. Integration of 2D lateral groundwater flow into the variable infiltration capacity (VIC) model and effects on simulated fluxes for different grid resolutions and aquifer diffusivities. Water. 13 (5), 663.
Schwarz, J., Mathijs, E., 2017. Globalization and the sustainable exploitation of scarce groundwater in coastal Peru. J. Clean. Prod. 147, 231–241.
Segond, M., Wheater, H.S., Onof, C., 2007. The significance of spatial rainfall representation for flood runoff estimation: A numerical evaluation based on the Lee catchment, UK. *J. Hydrol.* 347 (1–2), 116–131.

Spanoudaki, K., Stamou, A.I., Nanou-Giannarou, A., 2009. Development and verification of a 3-D integrated surface water–groundwater model. J. Hydrol. 375 (3–4), 410–427.
Sridhar, V., Billah, M.M., Hildreth, J.W., 2018. Coupled surface and groundwater hydrological modeling in a changing climate. Groundwater 56 (4), 618–635.
UK Centre for Ecology and Hydrology. 2020. *National River Flow Archive.* [Accessed 2021].
Valerio, A., Rajaram, H., Zagona, E., 2010. Incorporating groundwater-surface water interaction into river management models. Groundwater 48 (5), 661–673.
Wang, Z., Yang, Y., Wu, J., Sun, X., Lin, J., Wu, J., 2022. Multi-objective optimization of the coastal groundwater abstraction for striking the balance among conflicts of resource-environment-economy in Longkou City, China. *Water Res.* 211, 118045.
Whiteman, M.I., Seymour, K.J., Van Wonderen, J.J., Maginness, C.H., Hulme, P.J., Grout, M.W., Farrell, R.P., 2012. Start, development and status of the regulator-led national groundwater resources modelling programme in England and Wales. Geol. Soc. Lond. Spec. Publ. 364 (1), 19–37.
Xevi, E., Khan, S., 2005. A multi-objective optimisation approach to water management. J. Environ. Manage. 77 (4), 269–277.
Xu, X., Huang, G., Qu, Z., 2009. Integrating MODFLOW and GIS technologies for assessing impacts of irrigation management and groundwater use in the Hetao Irrigation District, Yellow River basin. Sci. China Ser. E: Technol. Sci. 52 (11), 3257–3263.
Zipper, S.C., Carah, J.K., Dillis, C., Gleeson, T., Kerr, B., Rohde, M.M., Howard, J.K., Zimmerman, J.K., 2019. Cannabis and residential groundwater pumping impacts on streamflow and ecosystems in Northern California. Environ. Res. Commun. 1 (12), 125005.